Journal Pre-proofs

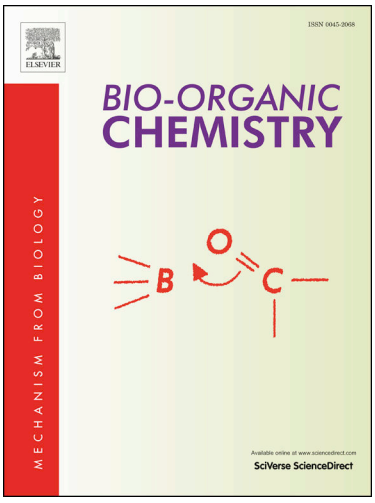

New Benzenesulfonamide Scaffold-Based Cytotoxic Agents: Design, Synthesis, cell viability, apoptotic activity and radioactive tracing studies

Yassin M. Nissan, Khaled O. Mohamed, Wafaa A. Ahmed, Dina M. Ibrahim, Marwa M. Sharaky, Tamer M. Sakr, Mohamed A. Motaleb, Ahmed Maher, Reem K. Arafa

PII: S0045-2068(19)31059-4
DOI: https://doi.org/10.1016/j.bioorg.2020.103577
Reference: YBIOO 103577

To appear in: *Bioorganic Chemistry*

Received Date: 3 July 2019
Revised Date: 11 December 2019
Accepted Date: 9 January 2020

Please cite this article as: Y.M. Nissan, K.O. Mohamed, W.A. Ahmed, D.M. Ibrahim, M.M. Sharaky, T.M. Sakr, M.A. Motaleb, A. Maher, R.K. Arafa, New Benzenesulfonamide Scaffold-Based Cytotoxic Agents: Design, Synthesis, cell viability, apoptotic activity and radioactive tracing studies, *Bioorganic Chemistry* (2020), doi: https://doi.org/10.1016/j.bioorg.2020.103577

New Benzenesulfonamide Scaffold-Based Cytotoxic Agents: Design, Synthesis, cell viability, apoptotic activity and radioactive tracing studies

Yassin M. Nissan[a,b], Khaled O. Mohamed[c], Wafaa A. Ahmed[d], Dina M. Ibrahim[e], Marwa M. Sharaky[d], Tamer M. Sakr[b,f,*], Mohamed A. Motaleb[g], Ahmed Maher[h], Reem K. Arafa[i,*]

[a]Pharmaceutical Chemistry Department, Faculty of Pharmacy, Cairo University, Kasr Elini St., Cairo 11562, Egypt

[b]Pharmaceutical Chemistry Department, Faculty of Pharmacy, October University for Modern Sciences and Arts (MSA), Giza, Egypt

[c]Pharmaceutical Organic Chemistry Department, Faculty of Pharmacy, Cairo University, Egypt

[d]National Cancer Institute, Cancer Biology Department, Cairo University, Egypt

[e]Faculty of Science, Cairo University, Cairo, Egypt

[f]Radioactive Isotopes and Generator Department, Hot Labs Center, Atomic Energy Authority, P.O. Box 13759, Cairo, Egypt

[g]Labeled Compounds Department, Hot Labs Center, Atomic Energy Authority, P.O. Box 13759, Cairo, Egypt

[h]Biochemistry Department, Faculty of Pharmacy, October University for Modern Sciences and Arts (MSA), Giza, Egypt

[i]Biomedical Sciences Program, University of Science and Technology, Zewail City of Science and Technology, 12578, Cairo, Egypt

Corresponding authors:

Prof. Reem K. Arafa
Biomedical Sciences Program
University of Science and Technology
Zewail City of Science and Technology
Ahmed Zewail Road
October Gardens, 6th of October City, Giza, Egypt, 12578
Mobile: +2-01002074028
E-mail: rkhidr@zewailcity.edu.eg

Associate Prof. Tamer M. Sakr
Radioactive Isotopes and Generator Department
Hot Labs Center
Atomic Energy Authority, Cairo, Egypt, 13759
Mobile: +2-01006884013
E-mail: tamer_sakr78@yahoo.com

Abstract

A new series of thiazolidinone (**5a-g**), thiazinone (**9a-g**) and dithiazepinone (**9a-g**) heterocycles bearing a benzenesulfonamide scaffold was synthesized. Cytotoxicity of these derivatives was assessed against MCF-7, HepG2, HCT-116 and A549 cancer cell lines and activity was compared to the known cytotoxic agents doxorubicin and 5-FU where the most active compounds displayed better to nearly similar IC_{50} values to the reference compounds. For assessing selectivity, the most active derivatives against MCF-7, **5b**, **5c** and **5e**, were also assessed against the normal breast cell line MCF-10 A where they demonstrated high selective cytotoxicity to cancerous cells over that to normal cells. Further, the effect of the most active compounds **5b-e** on MCF-7 and HepG2 cell cycle phase distribution was assessed and the tested sulfonamide derivatives were found to induce accumulation of cells in the <2n phase. To further confirm apoptosis induction, caspase 8 and 9 levels in MCF-7 and HepG2 were evaluated before and after treatment with compounds **5b-e** and were found to be significantly higher after exposure to the test agents. Since **5c** was the most active, its effect on the cell cycle regulation was confirmed where it showed inhibition of the CDK2/cyclin E1. Finally, *in vivo* biodistribution study using **radioiodinated-5c** revealed a significant uptake and targeting ability into solid tumor in a xenograft mouse model.

Key words: Benzenesulfonamide scaffold-based derivatives, cytotoxicity, caspase 8 and 9 levels, cell cycle phase distribution analysis.

1. Introduction

Cancer is the second leading cause of death worldwide. Statistical surveys show that 14.1 million new cases and 8.2 million cancer-related deaths were reported worldwide in 2012. [1] The choice of proper treatment depends on the patient's health condition and the goal of treatment. While surgery and radiation are treatment options, chemotherapy alone or in combination with the previously mentioned methods still holds a front line in treatment protocols [2]. Cytotoxic chemotherapeutics elicit their activity through preventing cell growth and/or inducing cell death (apoptosis) by inhibiting microtubule function, protein function, or DNA synthesis [3].

Those clinically used cytotoxins can be categorized as cell cycle-independent or cell cycle-dependent where they arrest cancer cell growth at specific cell cycle phases.[4] Molecular mechanisms underlying triggering of apoptotic pathway(s) involve activation and inactivation of key apoptotic proteins with an intricate interplay between the apoptotic machinery members. [5] Caspase 8, a cysteine protease which is a member of the apoptotic family proteins, is the initiator of a proteolytic cascade via the extrinsic pathway culminating in cell death [6,7]. Caspase 8 was found to be silenced in most patient tumor samples giving cancer cells a survival advantage [8]. Another important apoptosis linked protein is caspase 9 which is mainly induced by the mitochondria-linked intrinsic apoptotic pathway. Both the initiator caspases 8 and 9 are causatives of the successive activation of down-stream proteolytic executional caspases 3 and 7. [9] Cyclin-dependent kinase-2 (CDK2) is protein kinase responsible for cell cycle regulation and recently its overexpression is highly related to hyperproliferation [31] and in some cases recurrence and invasion. [32] Sulfonamide scaffold bearing aromatic/heterocyclic compounds have been frequently reported to possess cytotoxic activity. The observed anticancer activity was attributed to various modes of action such as carbonic anhydrase inhibition, cell cycle arrest, microtubule disruption, angiogenesis inhibition, apoptosis and autophagy induction, epigenetic modulation among others. [10-16]

In continuation to our quest for new cytotoxic agents based on the sulfonamide motif [17, 18], we herein present the synthesis and cytotoxic assessment of a new series of thiazolidinone, thiazinone and dithiazepinone derivatives bearing a benzenesulfonamide functionality. In addition, caspase 8 and 9 levels, cell cycle phase distribution analysis were determined for the most active compounds based on the apoptotic morphology of the cytotoxic agents treated cells upon microscopic evaluation. Finally, the CDK2 activity and the pharmacokinetic behavior of the most active compound **5c** was studied with the aid of radiolabeling technique to evaluate its targeting ability to solid tumor in tumor bearing mouse model [19-22].

2. Results and discussion

2.1. *Chemistry*

The synthesis routes of the target thiazolidinone (**5a-g**), thiazinone (**9a-g**) and dithiazepinone (**9a-g**) benzenesulfonamide derivatives is depicted in schemes 1 and 2. First, the key intermediate

chloroacetyl derivative **2** was synthesized from the thioureido derivative **1** through the reaction of the nucleophilic N-1 of thiourea with chloroacetyl chloride according to the reported method [23]. Compound **2** was further subjected to cyclization to the corresponding 1,3-thiazolidin-4-one derivative **3** upon refluxing in ethanol in the presence of catalytic amount of anhydrous sodium acetate [24]. Chemical structure of compound **3** was verified by elemental and spectral analyses. IR spectrum of compound **3** showed a characteristic band for C=O group at 1734 cm^{-1}. ^{1}H-NMR spectrum of compound **3** revealed a singlet at 4.17 ppm attributed to CH_2 of thiazolidinone ring. On the other hand, treatment of compound **2** with KSCN under reflux in absolute ethanol furnished the seven member 1,3,5-dithiazepine derivative **4**. Chemical structure of compound **4** was verified by elemental and spectral analyses. IR spectrum of compound **4** showed a band for C=O group at 1674 cm^{-1}. ^{1}H-NMR spectrum of compound **4** revealed a singlet at 4.03 ppm attributed to CH_2 group. The arylidene derivatives **5a-g** were synthesized from the thiazolidinone derivative **3** by condensing the active methylene group with several aromatic aldehydes in glacial acetic acid and a catalytic amount of anhydrous sodium acetate. Chemical structures of compounds **5a-g** were verified by elemental and spectral analyses. ^{1}H-NMR spectra of compounds **5a-g** revealed the absence of the singlet band at 4.17 ppm and the increment of aromatic proton bands confirming condensation. Applying the same procedure on the 1,3,5-dithiazepine derivative **4**, compounds **6a-g** were obtained. Chemical structures of compounds **6a-g** were verified by elemental and spectral analyses. ^{1}H-NMR spectra of compounds **6a-g** revealed the absence of the singlet band at 4.03 ppm and the increment of aromatic proton bands confirming condensation (Scheme 1).

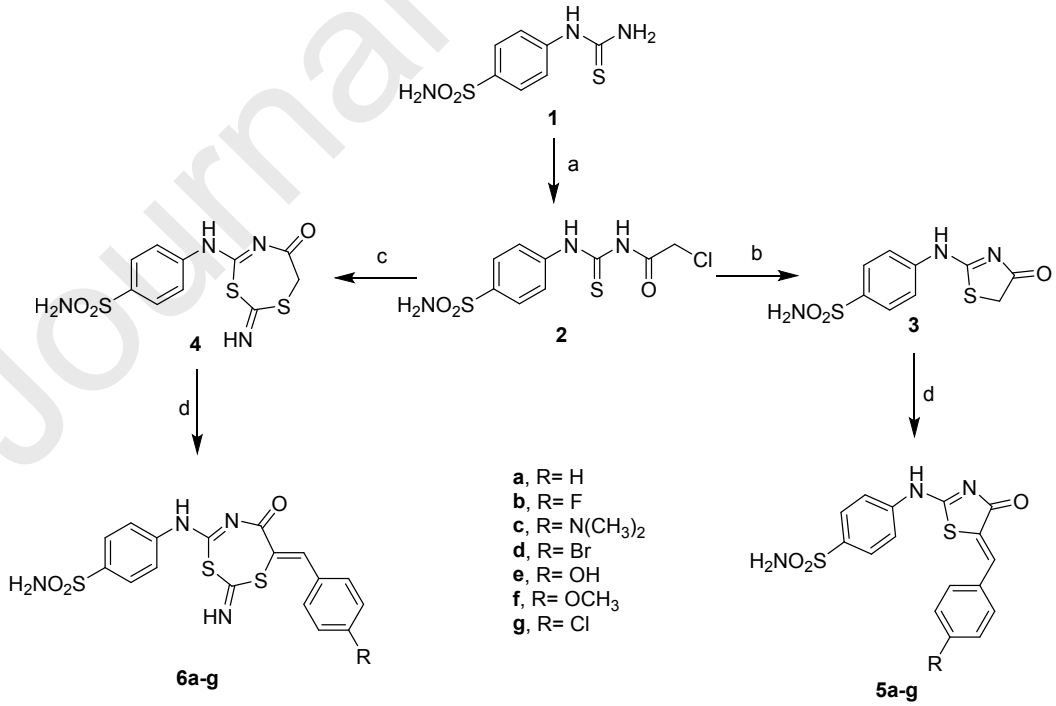

Scheme 1. Sovents and Reagents: a, Chlororacetyl chloride, DMF, anhydrous Na acetate; b, Ethanol, anhydrous Na acetate; c, Ethanol, KSCN; d, Aromatic aldehydes, Glacial Acetic Acid, anhydrous Na acetate

Several attempts were adopted to synthesize the six membered 1,3-thiazine derivative **8** from the thioureido derivative **1** through its reaction with 3-chloropropionyl chloride and further cyclization in ethanol but unfortunately compound **8** could not be obtained using this pathway. A different strategy was conducted through the reaction of 3-chloropropionyl chloride with KSCN in acetone followed by the addition of a solution sulfanilamide **7** in acetone which successfully furnished compound **8** in a good yield [25]. Chemical structure of compound **8** was verified by elemental and spectral analyses. IR spectrum of compound **8** showed bands 3377-3197 cm^{-1} for the NH and NH_2 groups, a band for C=O group at 1689 cm^{-1} and two bands at 1330, 1149 cm^{-1} for the SO_2 group. ^{1}H-NMR spectrum of compound **8** showed two triplets at 2.76 and 3.12 attributed to the $2CH_2$ groups. The arylidene derivatives **9a-g** could not be obtained by condensing the six membered 1,3-thiazine derivative **8** with aromatic aldehydes as done before in case of the thiazolidinone derivatives **5a-g** or the 1,3,5-dithiazepine derivatives **6a-g**. This lack of success in obtaining the target compounds can be attributed to the weakness of active methylene in this case due to the electron donating effect of the adjacent CH_2 and so more drastic condition needed to be applied. Neither increasing the reaction time to 72 hours nor the use of different bases such as piperidine, sodium ethoxide or even sodium hydroxide, succeeded to give the target compounds **9a-g**. In order to obtain the desired arylidene derivatives **9a-g**, fusion conditions were applied between the 1,3-thiazine derivative **8** and several aromatic aldehydes in an oil bath which finally furnished the target compounds in good yields [20]. Chemical structures of compounds **9a-g** were verified by elemental and spectral analyses. ^{1}H-NMR spectra of compounds **9a-g** revealed the disappearance of the two triplets at 2.76, 3.17 ppm and the appearance of new singlets in the range of 3.35-3.47 ppm corresponding to the CH_2 groups (Scheme 2).

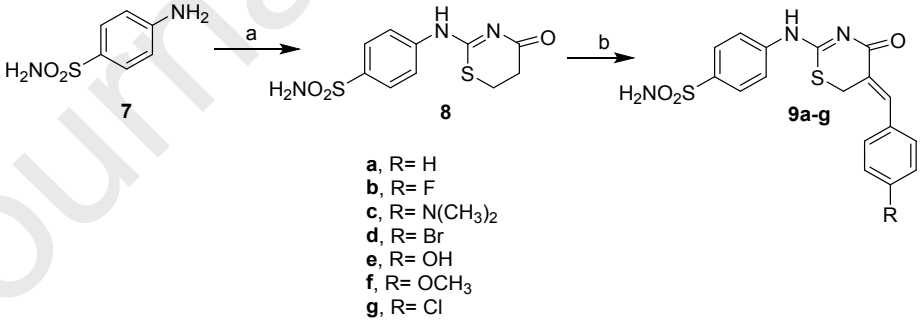

Scheme 2. Sovents and Reagents: a, 1,3-Chloropropionylchloride, KSCN, Acetone; b, Aromatic aldehydes, Glacial Acetic Acid, anhydrous Na acetate

2.2. Cytotoxicity Screening

Cytotoxicity of the newly synthesized compounds was assessed against breast, liver, colon and lung cancer cell lines MCF-7, HepG2, HCT-116 and A549, respectively using SRB method as previously described by Skehan *et al.* [26]. The half maximal inhibitory concentration values IC_{50}

of the tested compounds were calculated utilizing the prism program Version 5 (Table 1) from their respective dose response curves (Figures S22-S26 supplementary material).

While HCT-116 and A549 cell lines were responsive to all the tested compounds, MCF-7 and HepG2 were only sensitive to the cytotoxicity of a few derivatives.

For the HCT-116 colon cancer cell line, none of the tested compounds showed equal or better potency than the reference anticancer agent doxorubicin (IC_{50} = 0.058±0.02 µM). Yet, **5e** and **9d** exhibited almost equipotent cytotoxicity profile when compared to 5-FU (IC_{50} = 8.91±0.66, 6.93±0.51 and 7.7±1.25 µM, respectively). Also, **6f** and **9e** displayed almost a 2-fold potency increase relative to 5-FU (IC_{50} = 3.50±0.26 and 3.88±0.29 µM, respectively).

With regards to the A549 lung cancer cells, tested compounds showed excellent to moderate cytotoxicity profile (IC_{50} values between 1.69±0.11 and 157.17±10.48, 157.17±10.48 µM). Derivatives **6f** and **9d** were very potent where they were 5.4 and 2.7-fold more potent than 5-FU (IC_{50} 1.69±0.11, 3.36±0.23 and 9.27±0.69 µM, respectively). On the other hand, **5e**, **5g**, **6c**, **9c**, **9f** and **9g** all demonstrated high cytotoxicity (IC_{50} between 11.73±0.78 and 18.21±1.25 µM).

With respect to the MCF-7 breast cancer cell line, while all compounds were poorly active to inactive, derivatives **5b** and **5c** were between 4.5 and 2.7-fold more potent than both doxorubicin and 5-FU (IC_{50} = 0.37±0.005, 0.54±0.002, 1.50±0.02 and 1.70±0.03 µM, respectively).

Finally, HepG2 liver cancer cell line was mostly poorly sensitive to the cytotoxicity of the tested compounds. An exception was **5c** which was very cytotoxic being 3.7 times more potent than doxorubicin (IC_{50} = 0.24±0.012 and 0.90±0.12 µM, respectively). Also, **5b** and **5d** exhibited high cytotoxicity (IC_{50} = 1.58±0.031 and 2.28±0.120 µM, respectively); while **5e** was weakly active (IC_{50} >100 µM).

Table 1: *In vitro* cytotoxicity screening against cancer cell lines (data presented are IC_{50} µM ± SEM).

Compd. #	HCT-116*	A549	MCF-7	HepG2
5a	58.66±4.39	60.47±4.03	65.00±3.21	ND**
5b	53.73±4.02	57.78±3.85	0.37±0.005	1.58±0.031
5c	25.85±1.93	27.11±1.80	0.54±0.002	0.24±0.012
5d	27.32±2.04	26.30±1.75	ND	2.28±0.120
5e	8.91±0.66	11.73±0.78	17.04±0.65	>100
5f	22.16±1.66	32.61±2.17	78.30±4.21	ND
5g	12.38±0.92	13.25±0.91	71.70±3.58	ND
4	>100	95.71±6.28	ND	>100
6a	26.97±2.02	31.69±2.19	ND	ND
6b	18.85±1.41	29.70±2.05	>100	ND
6c	15.73±1.17	18.21±1.25	ND	ND
6d	45.35±3.39	50.27±3.47	ND	ND
6e	>100	>100	ND	ND
6f	3.50±0.26	1.69±0.11	ND	38.79±2.34
6g	10.00±0.74	9.38±0.64	ND	26.49±1.86
8	>100	>100	ND	ND

9a	10.00±0.74	30.96±2.14	ND	ND
9b	48.09±3.60	43.63±3.01	ND	ND
9c	51.40±3.84	13.07 ± 0.90	>100	ND
9d	6.93±0.51	3.36±0.23	>100	ND
9e	3.88±0.29	82.47±5.70	ND	ND
9f	96.81±7.24	17.92±1.23	ND	ND
9g	12.08±0.90	15.55±1.07	ND	ND
Dox	0.058±0.02	0.27±0.01	1.50±0.02	0.90±0.12
5-FU	7.7±1.25	9.27±0.69	1.70±0.03	38.50±2.12

* Results are average of triplicate experiments ± SEM

** ND = not detectable under the employed experimental conditions (> 1000 µM)

To further assess the selectivity profile of derivatives **5b**, **5c** and **5e**, their cytotoxic potential of against the normal breast cell line MCF-10A was evaluated (Table 2). All three test compounds demonstrated an IC_{50} of >100 µM. These results reflect the highly selective cytotoxicity of these agents (SI ranging between >5.8 to >270 fold) (dose response curves are provided in the supplementary material).

Table 2: *In vitro* cytotoxicity screening against normal breast cell line MCF-10 (data presented are IC_{50} µM).

Compd. #	MCF-10A*	SI**
5b	>100	>270
5c	>100	>185
5e	>100	>5.8

* Results are average of triplicate experiments

** SI (selectivity Index) = IC_{50} against MCF-10A/IC_{50} against MCF-7

2.3. Examination of cell viability under inverted microscope

All test compounds treated cells showed marked shrinkage, accumulation and observable apoptosis after 48 h of test agents' exposure (figures 1 and 2 for MCF-7 and HepG2 treated cells, respectively) compared to the untreated control cells. Moreover, the new compounds **5a-d** treated cells displayed higher rates of apoptosis than the standard reference drugs, doxorubicin and 5-FU, treated cells. To further confirm this observation, cell cycle analysis and caspases 8 and 9 cell concentrations were investigated as discussed in the following sections.

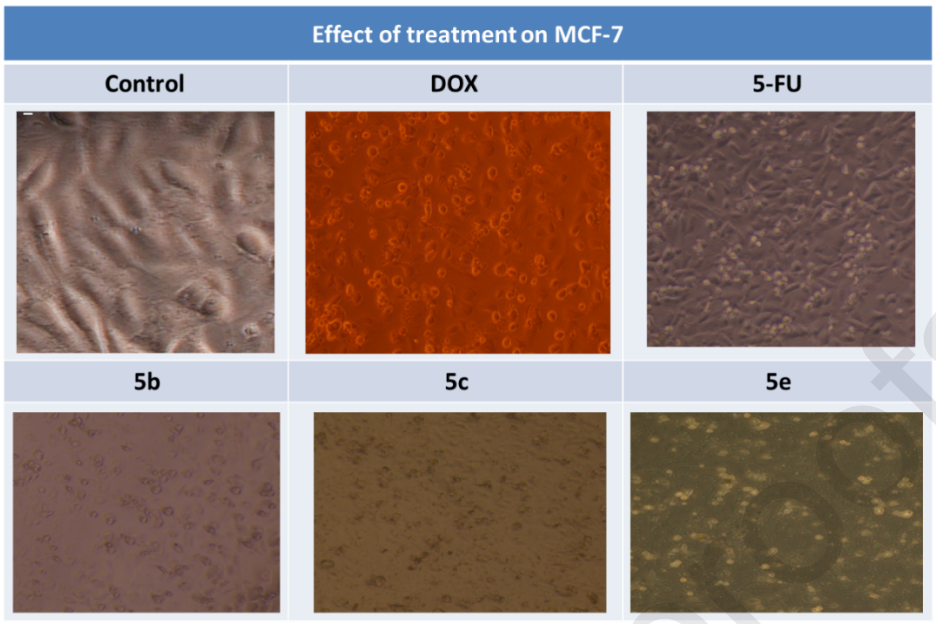

Fig. 1: Microscopic images of MCF-7 treated cells.

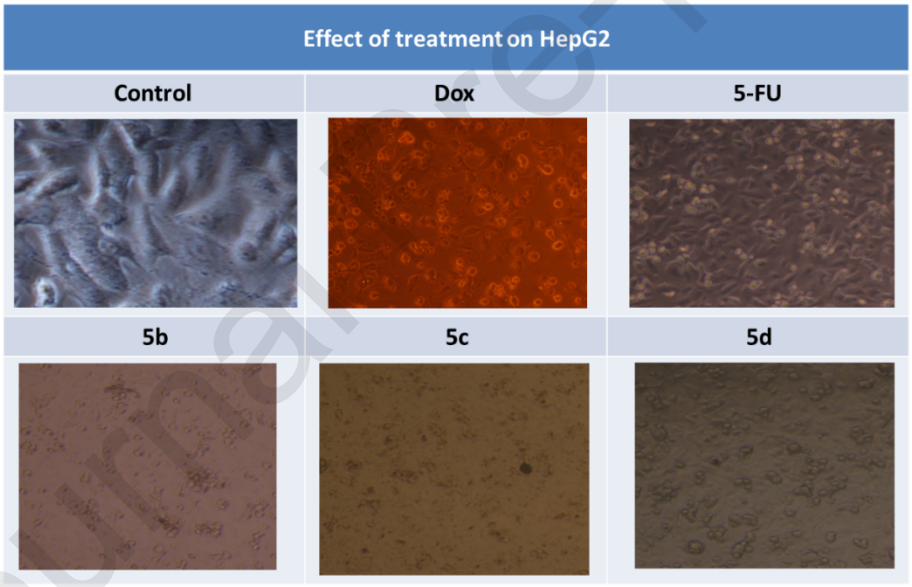

Fig. 2: Microscopic images of HepG2 treated cells.

2.4. Cell cycle analysis

To determine the effect of the new compounds on MCF-7 and HepG2 cell cycle phase distribution, cells were treated with the test agents for 24 h after which cell cycle histograms were obtained and results were analyzed (Figures 3 and 4).

Untreated MCF-7 cancer cells displayed a cell cycle population of 48%, 44.4% and 5.9% for the G0/G1, S and G2/M phases, respectively. Cell cycle analysis of **5b** treated MCF-7 breast cancer cells revealed the occurrence of population of 16.31% of the cells at the <2n phase, significant accumulation of cells at G0/G1 (74.4%) and a small percent of cells at the G2/M phase (1.6%) (Figure 3). On the other hand, **5c** cellular treatment led cells to accumulate at both <2n and G0/G1

phases (75 and 23%, respectively). Similarly, for derivative **5e**, major cell populations were found to exist at the <2n (54.5%) and G0/G1 (40%) phases.

5b treated MCF-7 cells (0.371 µM)	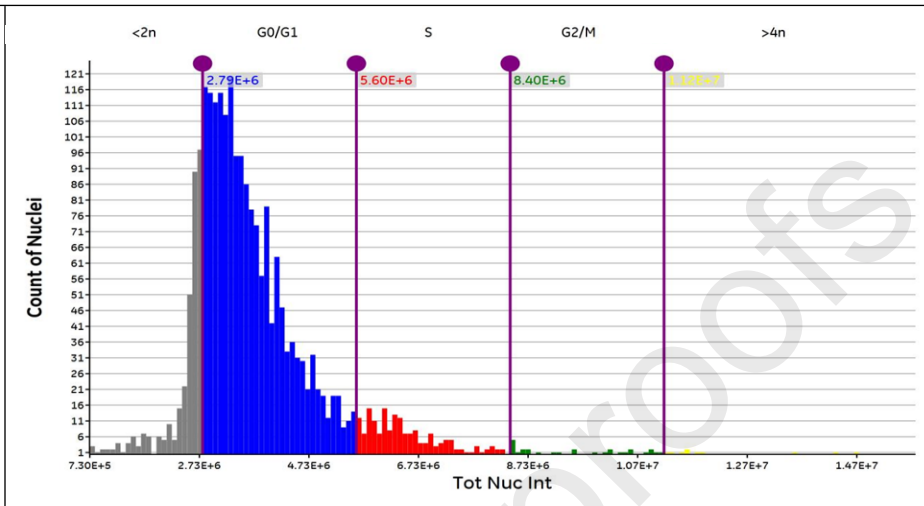
5c treated MCF-7 cells (0.547 µM)	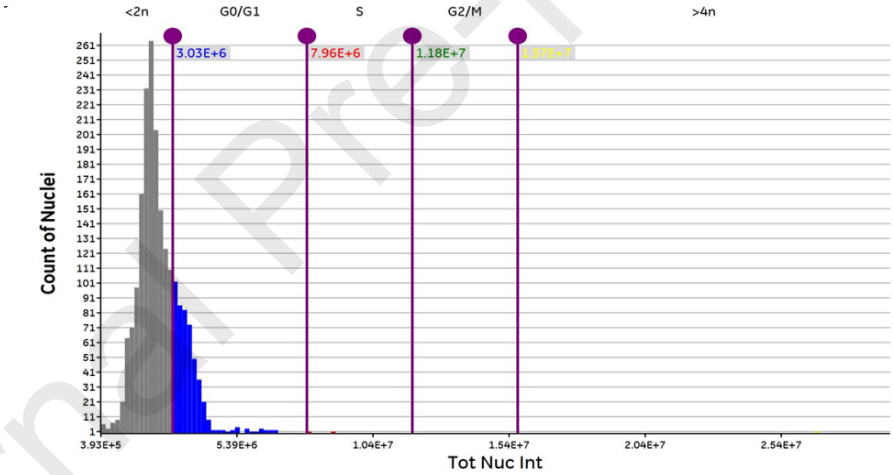
5e treated MCF-7 cells (17.04 µM)	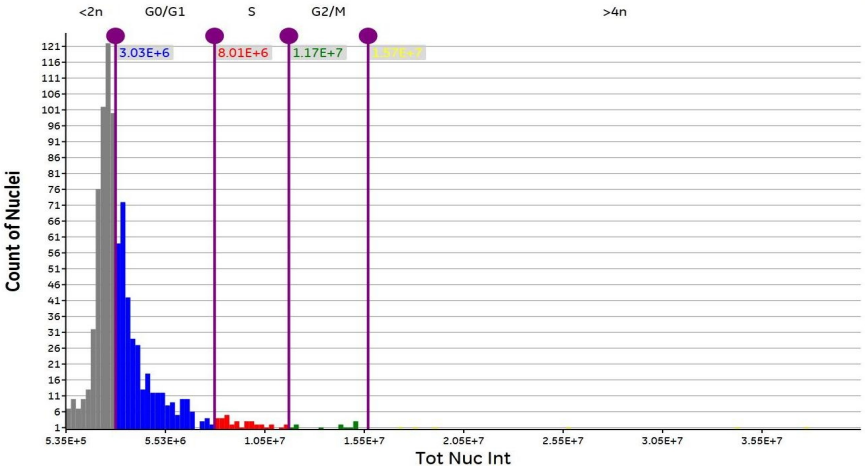

Untreated MCF-7 cells (negative control)	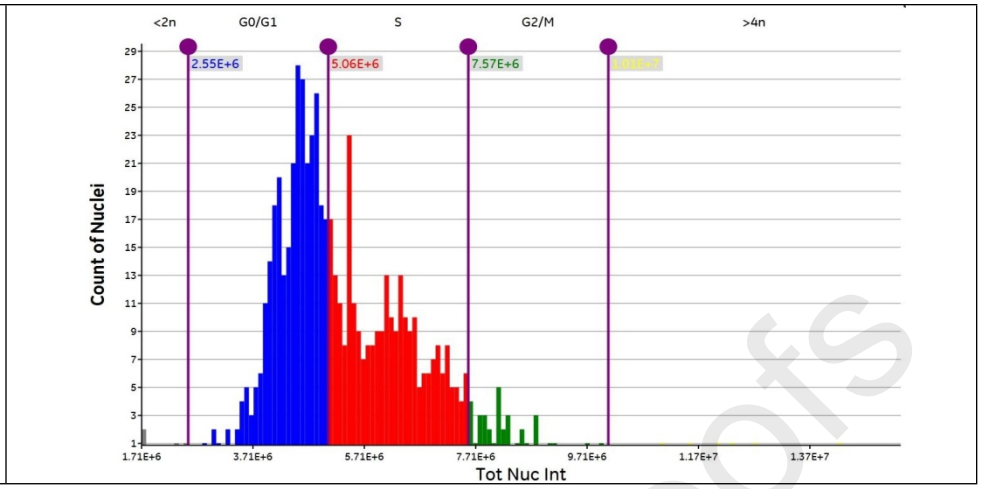

Fig. 3: Cell cycle analysis of MCF-7 **5b**, **5c** and **5e** treated cells *versus* untreated negative control cells.

Cell cycle analysis of untreated HepG2 cells showed that cells were distributed between the G0/G1, S and G2/M phases in 52.2%, 35.4 % and 5.1%, respectively (Figure 4). On the other hand, cell cycle analysis of HepG2 liver cancer cells revealed moderate <2n phase accumulation (28.1%), very high population at G0/G1 phase (67.9%) and poor existence at the G2/M phase (1.6%) for **5b** treated cells. Furthermore, **5c** treated cells showed a little higher <2n phase accumulation (41.3%), noticeable G0/G1 arrest (56.2%) and a small G2/M (1.7%) population. For derivative **5d**, it showed major accumulation of cells at both <2n (32%) and G0/G1 (65.3%) phases with a very small population at the G2/M phase (1.5%).

5b treated HepG2 cells (1.58 µM)	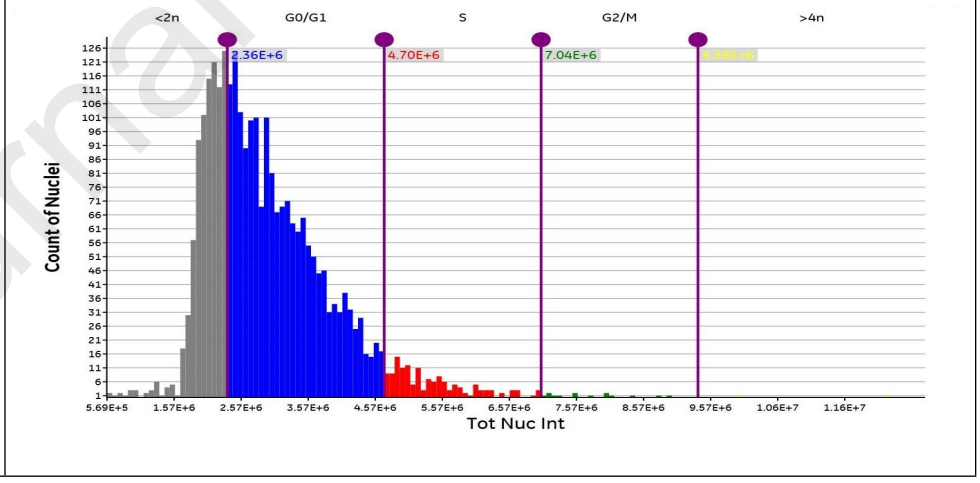

5c treated HepG2 cells (0.24 µM)	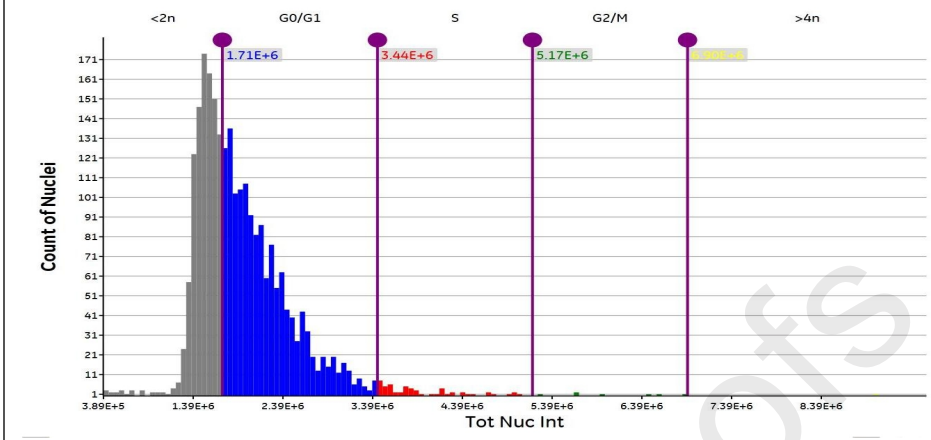
5d treated HepG2 cells (2.28 µM)	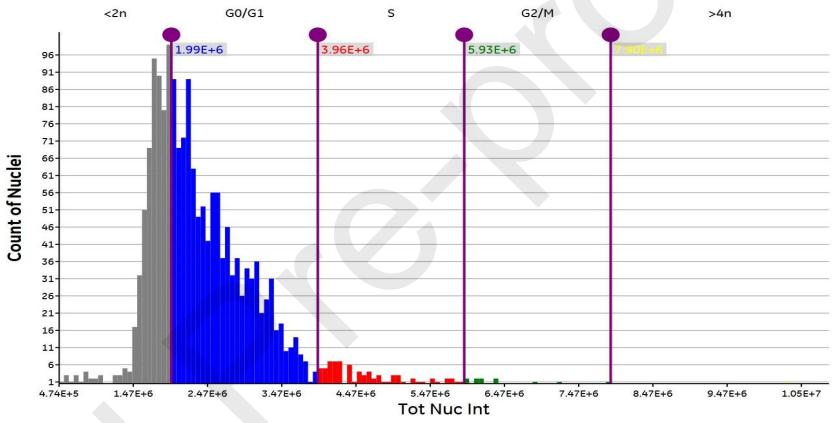
HepG2 untreated cells (negative control)	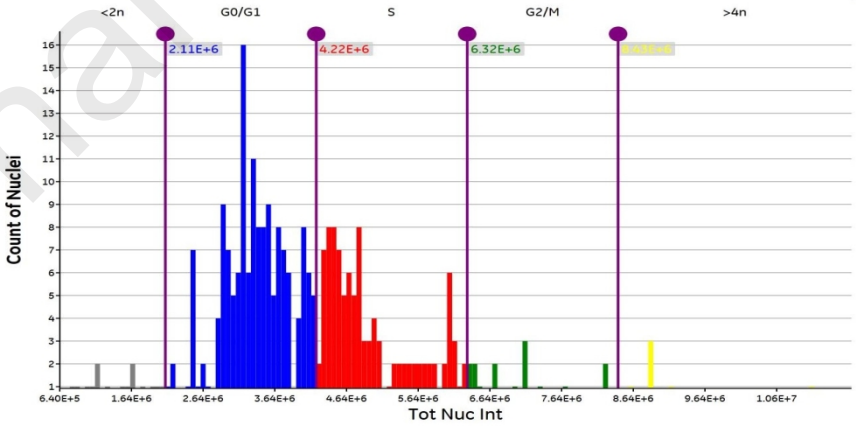

Fig. 4: Cell cycle analysis of HepG2 **5b**, **5c** and **5d** treated cells *versus* untreated negative control cells.

It can be concluded from this experiment that all test compounds induced accumulation of cells in the <2n phase and an induction of apoptosis in both MCF-7 and HepG2 treated cells. Also, the observed significant cell cycle arrest in the G0/G1 phase by exposure to the test agents is another indication of cell growth arrest which ultimately leads to apoptosis induction.

2.5. Caspase 8 and 9 levels

To further exploit the apoptotic behavior of MCF-7 and HepG2 treated cells, caspase 8 and 9 levels were examined in both cell lines (Tables 3 and 4).

Caspase 8 level was measured in MCF-7 and HepG2 cancer cell lines after treatment with the different test agents (**5b**,**c**&**e** for MCF-7; and **5b-d** for HepG2) at their respective IC_{50} concentrations and results were compared with doxorubicin and 5-FU as positive controls (Table 3). Experimental results showed significant increase in caspase 8 activity in both MCF-7 and HepG2 cancer cells treated with the test agents compared to the untreated control (p value <0.001) and both positive control drugs doxorubicin and 5-FU.

Table 3: Caspase 8 activity (absorbance at 400 or 405 nm).

Treatment	Conc. in MCF-7 cells*	P value	Conc. in HepG2 cells*	p value
Control	0.3±0.02	NA**	0.48±0.02	NA
Dox	0.75±0.03	<0.01	0.52±0.03	NS >0.05
5-FU	0.6±0.03	<0.05	0.7±0.02	<0.01
5b	1.02±0.04	<0.001	0.9±0.03	<0.001
5c	1.5±0.03	<0.001	1.3±0.05	<0.001
5d	NT***	NT	1.1±0.01	<0.001
5e	1.2±0.02	<0.001	NT	NT

* Results are average of triplicate experiments ± SEM
** NA = not applicable
*** NT = not tested

Similarly, capase-9 level was measured in MCF-7 and HepG2 cancer cell lines treated with the compounds under investigation (**5b-e**) at their respective IC_{50} values and were compared to controls (Table 4). MCF-7 test agents-treated cells showed extremely significant increase in caspase 9 enzymatic concentration compared to negative control and positive control (doxorubicin and 5-FU) treated counterparts. Analogous effect was observed for HepG2 treated cells.

Table 4: Caspase 9 activity (absorbance at 400 or 405 nm).

Treatment	Conc. in MCF-7 cells*	P value	Conc. in HepG2 cells*	P value
Control	0.38±0.02	NA**	0.21±0.02	NA
Dox	0.48±0.01	<0.01	0.31±0.01	<0.01
5-FU	0.4±0.02	NS >0.05	0.23±0.02	NS >0.05
5b	0.66±0.02	<0.05	0.28±0.01	<0.001
5c	0.78±0.01	<0.001	0.38±0.03	<0.001
5d	NT***	NT	0.36±0.01	<0.001
5e	0.56±0.01	<0.001	NT	NT

* Results are average of triplicate experiments ± SEM
** NA = not applicable
*** NT = not tested

2.6. CDK-2 inhibition activity for 5c

Compound **5c** was tested for inhibitory effect on CDK2 and showed moderate potency (IC_{50} = 56.97 ± 2 µM) (Figure 5). This could account for the cell cycle arrest in the G0/G1 phase [27] and in part account for the compound's high cytotoxicity.

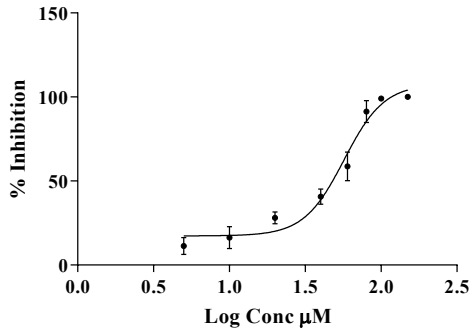

Fig. 5: Dose-dependent inhibitory effect of **5c** on CDK2.

2.7. Radiolabeling and in vivo biodistribution of radioiodinated-5c

Since compound **5c** showed the highest results in almost all conducted assays. It was selected for radiolabeling and biodistribution studies.

2.7.1. Radiosynthesis of radioiodinated-5c

The highest radiochemical yield (RCY) of **radioiodinated-5c** was 89.5±2.25%. Such maximum yield was obtained using 0.5 mg of compound **5c** and 50 mg chloramine-T. Radiolabeling reaction was done for 30 min reaction time at pH 4 at ambient temperature (27±3 °C). The *in-vitro* stability of **radioiodinated-5c** was up to 10 h.

2.7.2. Pharmacokinetic study of radioiodinated-5c

Results of **radioiodinated-5c** biodistribution pattern in Swiss albino mice with right tumor bearing thigh muscle are shown in **Table 5**. It was evident that there is a significant difference in uptake of **radioiodinated-5c** by the tumor tissues as represented by the tumor bearing right thigh muscle compared to non-cancerous tissues represented by the normal left thigh muscle at all-tested time intervals. Besides, the target to non-target ratio (T/NT) was greater than 1 at all-time intervals and reached its maximum value at 4 h post injection (T/NT= 4.66). Liver and intestine high radioactivity levels indicate that hepatobiliary pathway is the main excretion route of **radioiodinated-5c**. Low radioactivity levels of thyroid at different time intervals indicate the good *in-vivo* stability of **radioiodinated-5c**.

Table 5. Biodistribution of **radioiodinated-5c** in Swiss albino mice with right tumor bearing thigh muscle at different time intervals post-injection. (% ID/organ ± S.D., n = 5).

Organs	15 min	60 min	2 h	4 h
Blood	47.07±3.78	28.84±3.51	31.69±3.55	16.93±2.43
Kidneys	5.73±0.47	4.34±0.73	4.21±0.52	6.88±0.75
Liver	16.03±1.90	26.82±2.67	28.86±3.5	32.95±4.21
Spleen	0.66±0.12	1.22±0.03	1.56±0.18	1.37±0.13
Intestine	8.62±0.91	12.15±1.63	14.45±1.32	24.57±3.71
Stomach	1.39±0.05	4.88±0.42	5.01±0.68	4.07±0.44
Lungs	3.88±0.7	1.16±0.05	2.15±0.18	2.23±0.09
Heart	1.02±0.03	0.34±0.09	0.34±0.04	0.24±0.01
Bone	2.79±0.17	8.78±0.94	3.09±0.21	2.18±0.24
Thyroid	1.34±0.22	1.87±0.11	2.30±0.35	1.90±0.22
Normal left thigh muscle	12.82±0.99	11.48±1.23	8.62±0.89	8.59±0.83
Tumor right thigh muscle	20.17±1.86	27.36±3.65	29.38±3.51	40.10±5.99
T/NT	1.57	2.38	3.41	4.66

3. Conclusion

Twenty-one new compounds belonging to the thiazolidinone (**5a-g**), thiazinone (**9a-g**) and dithiazepinone (**9a-g**) heterocycles bearing a benzenesulfonamide scaffold were synthesized. These derivatives were found to display promising cytotoxicity against MCF-7, HepG2, HCT-116 and A549 cancer cell lines and activity as compared to the known cytotoxic agents doxorubicin and 5-FU. The IC_{50} values for compounds **5b** and **5c** on MCF-7 cell line were 0.37 and 0.54 µM, respectively, while those for compounds **5b, 5c** and **5d** on HepG2 cell line were 1.58, 0.24 and 2.28 µM, respectively. Cytotoxicity of the **5b**, **5c** and **5e** towards MCF-10A, normal breast cell line, was also assessed and all three compounds were found to be selectively much more toxic to MCF-7 breast cancer cell line and far less toxic to MCF-10A. Additionally, cell cycle analysis showed that the most active compounds **5b-e** were able to disrupt MCF-7 and HepG2 cell cycle phase distribution inducing cellular accumulation in the <2n phase which is a hall-mark of apoptosis. Furthermore, evaluation of caspase 8 and 9 levels in MCF-7 and HepG2 before and after treatment with the most active compounds **5b-e** demonstrated a significant increase in the concentration of these apoptotic proteins which is a second hall-mark for programmed cell death induction. Compound **5c** has increased the level of caspase 8 by 5 folds in MCF-7 cells and almost for folds in HepG2 cells. The same compound has also increased the level of caspase 9 by almost two folds in HepG2 cells. Testing compound **5c** showed it had some inhibitory effect on CDK2 explaining the accumulation of treated cells in the G0/G1 phase. The IC_{50} value for this inhibition was 56.97 µM. Finally, pharmacokinetic study of the ^{125}I **radioiodinated-5c** was performed and biodistribution results showed a significant high accumulation of radioactivity in cancer bearing thigh muscle compared to the normal thigh muscle (high T/NT) that reached 4.66 in 4 hours. In

conclusion, the derivative **5c** displays the qualities of a promising lead compound, which can be adopted for further optimization.

4. Experimental

4.1. Chemistry

Melting points were determined on Electro thermal Stuart 5MP3 digital melting point apparatus and were uncorrected. Elemental microanalyses were performed at the micro analytical center, Al-Azhar University, Cairo, Egypt. IR spectra were recorded on a Bruker Fourier transform (FT)-IR spectrophotometer as KBr discs. NMR spectra (in DMSO-d_6) were recorded on Bruker AC-300 Ultra Shield NMR spectrometer (Bruker, Flawil, Switzerland, δ ppm) at 400 MHz using TMS as internal Standard and peak multiplicities are designed as follows: s, singlet; d, doublet; t, triplet; m, multiplet. Silica gel used for column chromatography was obtained from Fluka, 70-230 mesh thin layer chromatography was carried out on silica gel TLC plates with fluorescence indicator (F_{254}).

4.1.1. 2-Chloro-N-(4-sulfamoylphenyl)acetamide **2**

The target compound was prepared according the reported method. Yield: 63%; m.p: 207–208 °C (as reported). [23]

4.1.2. 4-(4-Oxo-4,5-dihydrothiazol-2-ylamino)benzenesulfonamide **3**

To a solution of the choloro derivative **2** (0.01 mol, 2.48 g) in absolute ethanol (20 mL), a catalytic amount of anhydrous sodium acetate (0.5 g) was added and the reaction mixture was refluxed for three hours. The white precipitate formed was filtered, dried, washed with hot ethanol and crystallized from DMF/H_2O to give white powder of **3**.

Yield: 68%; m.p.: 213–215 °C; IR (KBr) (cm^{-1}): 3390, 3204 (NH, NH_2), 3050-3015 (CH arom.), 1734 (C=O), 1344, 1163 (SO_2); ^{1}HNMR (400 MHz, DMSO-d_6) δ: 4.17 (s, 2H, CH_2), 7.47 (s, 2H, NH_2SO_2, D_2O exchangeable), 7.47-7.50 (d, 2H, Ar H), 7.91-7.93 (d, 2H, Ar H), 9.38 (s, 1H, NH, D_2O exchangeable); ^{13}CNMR (100.63 MHz, DMSO-d_6) δ: 34.30(1), 126.75(2), 129.72(2), 138.41(1), 144.13(1), 158.34(1), 171.97(1); Anal. Calcd. for $C_9H_9N_3O_3S_2$ (Mwt. 271.32): C, 39.84; H, 3.34; N, 15.49; found: C, 39.91; H, 3.38; N, 15.63.

4.1.3. 4-(2-Imino-6-oxo-6,7-dihydro-1,3,5-dithiazepin-4-ylamino)benzenesulfonamide **4**

To a solution of the chloro derivative **2** (0.01 mol, 2.48 g) in absolute ethanol (20 mL), KSCN (0.01 mol, 0.97 g) was added and the reaction mixture was refluxed for five hours. The canary yellow precipitate formed was filtered, dried, washed with hot ethanol and crystallized from DMF/H_2O to give yellow powder of **4**.

Yield: 75%; m.p.: 260–262 °C; IR (KBr) (cm^{-1}): 3360, 3271 (NH, NH_2), 3051-3001 (CH arom.), 1674 (C=O), 1296, 1151(SO_2); ^{1}HNMR (400 MHz, DMSO-d_6) δ: 4.03 (s, 2H, CH_2), 7.10 (s, 2H, NH_2SO_2, D_2O exchangeable), 7.31 (d, 2H, Ar H), 7.82 (d, 2H, Ar H), 11.51 (s, 1H, NH, D_2O exchangeable),

11.92 (s, 1H, NH, D_2O exchangeable); ^{13}CNMR (100.63 MHz, DMSO-d_6) δ: 19.02(1), 120.40(2), 121.77(2), 127.26(2), 140.05(2), 152(1); Anal. Calcd. for $C_{10}H_{10}N_4O_3S_3$ (Mwt. 330.41): C, 36.35; H, 3.05; N, 16.96; found C, 36.44; H, 3.03; N, 17.08.

4.1.4. General procedure for preparation of compounds **5a-g**

To a solution of compound **3** (0.01 mol, 2.71 g) in glacial acetic acid (20 mL), catalytic amount of anhydrous sodium acetate (0.5 g) was added. After complete dissolution, the appropriate aromatic aldehyde (0.01 mol) was added and the reaction mixture was refluxed for 6-8 hours. The precipitate formed was filtered, dried, washed with hot ethanol and crystallized from DMF/H_2O to give **5a-g**, respectively.

4.1.4.1. 4-(5-Benzylidene-4-oxo-4,5-dihydrothiazol-2-ylamino)benzenesulfonamide **5a**

Yield: 72%; m. p.: < 300 °C; IR (KBr) (cm^{-1}): 3313, 3246 (NH, NH_2), 3050-3010 (CH arom.), 1678 (C=O), 1319, 1153 (SO_2); Anal. Calcd. for $C_{16}H_{13}N_3O_3S_2$ (Mwt. 359.42): C, 53.47; H, 3.65; N, 11.69; found C, 53.54; H, 3.68; N, 11.77.

4.1.4.2. 4-(5-(4-Fluorobenzylidene)-4-oxo-4,5-dihydrothiazol-2-ylamino)benzenesulfonamide **5b**

Yield: 65%; m.p.: 279–281°C; IR (KBr) (cm^{-1}): 3317, 3242 (NH, NH_2), 3055-3010 (CH arom.), 1683 (C=O), 1338, 1157 (SO_2); ^{1}HNMR (400 MHz, DMSO-d_6) δ: 7.20 (s, 2H, NH_2SO_2, D_2O exchangeable), 7.22-7.85 (m, 8H, Ar H), 7.95 (s, 1H, CH=C), 12.42 (s, 1H, NH, D_2O exchangeable); ^{13}CNMR (100.63 MHz, DMSO-d_6) δ: 116.80(2), 120.78(1), 121.98(2), 122.82(1), 127.48(1), 127.75(2), 129.39(1), 130.35(1), 132.65(2), 140.12(1), 140.65(1), 161.82(1); Anal. Calcd. for $C_{16}H_{12}FN_3O_3S_2$ (Mwt. 377.41): C, 50.92; H, 3.20; N, 11.13; found C, 51.03; H, 3.24; N, 11.26.

4.1.4.3. 4-(5-(4-(Bimethylamino)benzylidene)-4-oxo-4,5-dihydrothiazol-2-ylamino)benzene-sulfonamide **5c**

Yield: 55%; m.p.: 285–287 °C; IR (KBr) (cm^{-1}): 3356, 3238 (NH, NH_2), 3122-3043 (CH arom.), 2922 (CH aliph.), 1670 (C=O), 1319, 1155 (SO_2); ^{1}HNMR (400 MHz, DMSO-d_6) δ: 3.04 (s, 6H, $N(CH_3)_2$), 6.80-6.84 (m, 3H, Ar H), 7.20 (s, 2H, NH_2SO_2, D_2O exchangeable), 7.35-7.50 (m, 3H, Ar H), 7.66-7.96 (d, 2H, Ar H), 7.98 (s, 1H, CH=C), 12.27 (s, 1H, NH, D_2O exchangeable); ^{13}CNMR (100.63 MHz, DMSO-d_6) δ: 40.00(2), 112.55(2), 120.20(1), 126.98(2), 129.22(2), 132.17(2), 132.96(2), 135.06(1), 144.80(1), 152.19(1), 165.57(1), 167.45(1); Anal. Calcd. for $C_{18}H_{18}N_4O_3S_2$ (Mwt. 402.49): C, 53.71; H, 4.51; N, 13.92; found C, 53.87; H, 4.57; N, 14.08.

4.1.4.4. 4-(5-(4-Bromobenzylidene)-4-oxo-4,5-dihydrothiazol-2-ylamino)benzenesulfonamide **5d**

Yield: 55%; m.p. < 300 °C; IR (KBr) (cm^{-1}): 3332, 3201 (NH, NH_2), 3043-3010 (CH arom.), 1670 (C=O), 1317, 1155 (SO_2); ^{1}HNMR (400 MHz, DMSO-d_6) δ: 7.19 (d, 2H, Ar H), 7.21 (s, 2H, NH_2SO_2, D_2O exchangeable),7.44 (d, 2H, Ar H), 7.58 (d, 2H, Ar H), 7.90 (d, 2H, Ar H), 7.95 (s, 1H, CH=C), 12.59 (s, 1H, NH, D_2O exchangeable); ^{13}CNMR (100.63 MHz, DMSO-d_6) δ: 120.90(1), 121.98(2),

123.88(2), 127.76(2), 129.22(1), 132.00(2), 132.87(2), 140.68(2), 167.79(1), 171.83(1); Anal. Calcd. for $C_{16}H_{12}BrN_3O_3S_2$ (Mwt. 438.32): C, 43.84; H, 2.76; N, 9.59; found C, 43.91; H, 2.74; N, 9.67.

4.1.4.5. 4-(5-(4-Hydroxybenzylidene)-4-oxo-4,5-dihydrothiazol-2-ylamino)benzenesulfonamide **5e**

Yield: 52%; m.p. < 300 °C; IR (KBr) (cm^{-1}): 3446 (OH), 3346, 3255 (NH, NH_2), 3041-3010 (CH arom.), 1670 (C=O), 1311, 1151 (SO_2); ^{1}HNMR (400 MHz, DMSO-d_6) δ: 6.87 (d, 2H, Ar H), 7.19 (d, 2H, Ar H), 7.21 (s, 2H, NH_2SO_2, D_2O exchangeable), 7.58 (d, 2H, Ar H), 7.92 (d, 2H, Ar H), 7.95 (s, 1H, CH=C), 10.20 (s, 1H, OH, D_2O exchangeable), 12.37 (s,1H,NH, D_2O exchangeable); ^{13}CNMR (100.63 MHz, DMSO-d_6) δ: 116.76(4), 122.00(2), 124.56(1), 127.74(2), 130.98(1), 132.48(2), 140.45(1), 151.50(1), 159.99(1), 168.10(1); Anal. Calcd. for $C_{16}H_{13}N_3O_4S_2$ (Mwt. 375.42): C, 51.19; H, 3.49; N, 11.19; found C, 51.32; H, 3.54; N, 11.26.

4.1.4.6. 4-(5-(4-Methoxybenzylidene)-4-oxo-4,5-dihydrothiazol-2-ylamino)benzenesulfonamide **5f**

Yield: 67%; m.p. < 300°C; IR (KBr) (cm^{-1}): 3334, 3248 (NH, NH_2), 3045-3020 (CH arom.), 2926 (CH aliph.), 1678 (C=O), 1319, 1153 (SO_2); Anal. Calcd. for $C_{17}H_{15}N_3O_4S_2$ (Mwt. 389.45): C, 52.43; H, 3.88; N, 10.79; found C, 52.57; H, 3.92; N, 10.87.

4.1.4.7. 4-(5-(4-Chlorobenzylidene)-4-oxo-4,5-dihydrothiazol-2-ylamino)benzenesulfonamide **5g**

Yield: 52%; m.p. < 300 °C; IR (KBr) (cm^{-1}): 3325, 3250 (NH, NH_2), 3090-3025 (CH arom.), 1670 (C=O), 1319, 1157 (SO_2); Anal. Calcd. for $C_{16}H_{12}ClN_3O_3S_2$ (Mwt. 393.87): C, 48.79; H, 3.07; N, 10.67; found C, 48.88; H, 3.11; N, 10.82.

4.1.5. General procedure for prepration of compounds **6a-g**

To a solution of compound **4** (0.01 mol, 3.30 g) in glacial acetic acid (20 mL), catalytic amount of anhydrous sodium acetate (0.5 g) was added. After complete dissolution, the appropriate aromatic aldehyde (0.01 mol) was added and the reaction mixture was refluxed for 6-8 hours. The precipitate formed was filtered, dried, washed with hot ethanol and crystallized from DMF/H_2O to give **6a-g**, respectively.

4.1.5.1. 4-(7-Benzylidene-2-imino-6-oxo-6,7-dihydro-1,3,5-dithiazepin-4-ylamino)-benzene-sulfonamide **6a**

Yield: 80%; m.p. < 300°C; IR (KBr) (cm^{-1}): 3315-3197 (2NH, NH_2), 3090-3039 (CH arom.), 1676 (C=O), 1319, 1155 (SO_2); ^{1}HNMR (400 MHz, DMSO-d_6) δ: 7.19 (d, 2H, Ar H) , 7.21 (d, 2H, Ar H), 7.26 (s, 2H, NH_2SO_2, D_2O exchangeable), 7.59-7.85 (m, 5H, Ar H), 7.95 (s, 1H, CH=C), 11.93 (s, 1H, NH, D_2O exchangeable), 12.53 (s, 1H, NH, D_2O exchangeable); ^{13}CNMR (100.63 MHz, DMSO-d_6) δ ppm: 120.92(2), 121.99(2), 127.75(2), 129.76(2), 130.19(2), 130.48(2), 133.68(1), 140.63(1),

152.50(1), 161.00(1), 166.34(1); Anal. Calcd. for $C_{17}H_{14}N_4O_3S_3$ (Mwt. 418.51): C, 48.79; H, 3.37; N, 13.39; found C, 48.89; H, 3.40; N, 13.46.

4.1.5.2. 4-(7-(4-Fluorobenzylidene)-2-imino-6-oxo-6,7-dihydro-1,3,5-dithiazepin-4-ylamino)-benzenesulfonamide **6b**

Yield 70%; m.p. < 300 °C; IR (KBr) (cm^{-1}): 3317-3199 (2NH, NH_2), 3085-3045 (CH arom.), 1681 (C=O), 1317, 1159 (SO_2); ^{1}HNMR (400 MHz, DMSO-d_6) δ: 7.19 (d, 2H, Ar H), 7.21 (d, 2H, Ar H), 7.31 (s, 2H, NH_2SO_2, D_2O exchangeable), 7.58-7.86 (m, 4H, Ar H), 7.95 (s, 1H, CH=C), 11.53 (s, 1H, NH, D_2O exchangeable), 12.49 (s, 1H, NH, D_2O exchangeable); ^{13}CNMR (100.63 MHz, DMSO-d_6) δ: 116.79(2), 120.89(1), 121.98(2), 127.75(2), 129.37(1), 130.33(1), 132.64(2), 140.65(2), 151.19(1), 161.82(1), 164.29(1), 167.95(1); Anal. Calcd. for $C_{17}H_{13}FN_4O_3S_3$ (Mwt. 436.50); C, 46.78; H, 3.00; N, 12.84; found C, 46.89; H, 3.02; N, 12.89.

4.1.5.3. 4-(7-(4-(Dimethylamino)benzylidene)-2-imino-6-oxo-6,7-dihydro-1,3,5-dithiazepin-4-ylamino)benzenesulfonamide **6c**

Yield: 64%; m.p. < 300 °C; IR (KBr) (cm^{-1}): 3300-3197 (2NH, NH_2), 3080-3039 (CH arom.), 2953 (CH aliph.), 1680 (C=O), 1321, 1155 (SO_2); ^{1}HNMR (400 MHz, DMSO-d_6) δ: 2.98 (s, 6H, $N(CH_3)_2$), 6.80 (d, 2H, Ar H), 7.20 (d, 2H, Ar H), 7.35 (s, 2H, NH_2SO_2, D_2O exchangeable),7.55-7.85 (m, 4H, Ar H), 7.96 (s, 1H, CH=C), 11.73 (s, 1H, NH, D_2O exchangeable), 12.26 (s, 1H, NH, D_2O exchangeable); ^{13}CNMR (100.63 MHz, DMSO-d_6) δ: 39.79(2), 112.55(2), 119.68(2), 120.76(2), 122.75(2), 127.75(2), 132.16(2), 143.73(2), 152.19(1), 157.86(1), 167.48(1); Anal. Calcd. for $C_{19}H_{19}N_5O_3S_3$ (Mwt. 461.58): C, 49.44; H, 4.15; N, 15.17; found C, 49.53; H, 4.19; N, 15.28.

4.1.5.4. 4-(7-(4-Bromobenzylidene)-2-imino-6-oxo-6,7-dihydro-1,3,5-dithiazepin-4-ylamino)-benzenesulfonamide **6d**

Yield: 58%; m.p. < 300 °C; IR (KBr) (cm^{-1}): 3334-3195 (2NH, NH_2), 3091-3035 (CH arom.), 1670 (C=O), 1317, 1155 (SO_2); ^{1}HNMR (400 MHz, DMSO-d_6) δ: 7.19 (d, 2H, Ar H), 7.37 (s, 2H, NH_2SO_2, D_2O exchangeable), 7.46 (d, 2H, Ar H), 7.68-7.89 (m, 4H, Ar H), 7.95 (s, 1H, CH=C), 11.97 (s, 1H, NH, D_2O exchangeable), 12.61 (s, 1H, NH, D_2O exchangeable); ^{13}CNMR (100.63 MHz, DMSO-d_6) δ: 121.93(2), 123.88(2), 127.76(2), 132.02(2), 132.76(4), 140.66(2), 152.59(1), 168.80(1), 172.00(1); Anal. Calcd. for $C_{17}H_{13}BrN_4O_3S_3$ (Mwt. 497.41): C, 41.05; H, 2.63; N, 11.26; found C, 41.21; H, 2.60; N, 11.39.

4.1.5.5. 4-(7-(4-Hydroxybenzylidene)-2-imino-6-oxo-6,7-dihydro-1,3,5-dithiazepin-4-ylamino)-benzenesulfonamide **6e**

Yield: 65%; m.p. < 300 °C; IR (KBr) (cm^{-1}): 3440 (OH), 3360-3271 (2NH, NH_2), 3049-3001 (CH arom.), 1674 (C=O), 1332, 1149 (SO_2); ^{1}HNMR (400 MHz, DMSO-d_6) δ: 6.88-7.19 (m, 4H, Ar H), 7.21 (s, 2H, NH_2SO_2, D_2O exchangeable), 7.31 - 7.74 (m, 4H, Ar H), 7.82 (s, 1H, CH=C), 10.20 (s, 1H, OH, D_2O exchangeable), 11.48 (s, 1H, NH, D_2O exchangeable), 11.90 (s, 1H, NH, D_2O

exchangeable); ^{13}CNMR (100.63 MHz, DMSO-d_6) δ: 116.76(2), 120.49(2), 121.83(2), 127.52(2), 132.47(2), 140.12(4), 151.81(1), 160.12(1), 172.23(1); Anal. Calcd. for $C_{17}H_{14}N_4O_4S_3$ (Mwt. 434.51): C, 46.99; H, 3.25; N, 12.89; found C, 47.06; H, 3.28; N, 13.02.

4.1.5.6. 4-(2-Imino-7-(4-methoxybenzylidene)-6-oxo-6,7-dihydro-1,3,5-dithiazepin-4-ylamino)-benzenesulfonamide **6f**

Yield: 58%; m.p. < 300 °C; IR (KBr) (cm^{-1}): 3325-3197 (2NH, NH_2), 3090-3045 (CH arom.), 2926 (CH aliph.), 1668 (C=O), 1328, 1157 (SO_2); ^{1}HNMR (400 MHz, DMSO-d_6) δ: 3.83 (s, 3H, OCH_3), 7.05-7.21 (m, 4H, Ar H), 7.36 (s, 2H, NH_2SO_2, D_2O exchangeable),7.47-7.85 (m, 4H, Ar H), 7.95 (s, 1H, CH=C), 11.82 (s, 1H, NH, D_2O exchangeable), 12.42 (s, 1H, NH, D_2O exchangeable); ^{13}CNMR (100.63 MHz, DMSO-d_6) δ: 55.90(1), 115.36(4), 122.00(2), 127.73(2), 132.17(4), 140.55(2), 151.00(1), 162.33(1), 171.00(1); Anal. Calcd. for $C_{18}H_{16}N_4O_4S_3$ (Mwt. 448.54): C, 48.20; H, 3.60; N, 12.49; found C, 48.28; H, 3.64; N, 12.63.

4.1.5.7. 4-(7-(4-Chlorobenzylidene)-2-imino-6-oxo-6,7-dihydro-1,3,5-dithiazepin-4-ylamino)-benzenesulfonamide **6g**

Yield: 63%; m.p. < 300 °C; IR (KBr) (cm^{-1}): 3325-3201 (2NH, NH_2), 3090-3047 (CH arom.), 1670 (C=O), 1319, 1159 (SO_2); ^{1}HNMR (400 MHz, DMSO-d_6) δ: 7.19 (d, 2H, Ar H), 7.37 (s, 2H, NH_2SO_2, D_2O exchangeable), 7.55 (d, 2H, Ar H), 7.68-7.89 (m, 4H, Ar H), 7.95 (s, 1H, CH=C), 11.85 (s, 1H, NH, D_2O exchangeable), 12.57 (s, 1H, NH, D_2O exchangeable); ^{13}CNMR (100.63 MHz, DMSO-d_6) δ: 121.97(2), 127.75(2), 129.84(4), 131.85(2), 135.00(2), 140.68(2), 152.00(1), 163.50(1), 169.00(1); Anal. Calcd. for $C_{17}H_{13}ClN_4O_3S_3$ (Mwt. 452.96): C, 45.08; H, 2.89; N, 12.37; found C, 45.15; H, 2.87; N, 12.49.

4.1.6. 4-(4-Oxo-5,6-dihydro-4H-1,3-thiazin-2-ylamino)benzenesulfonamide **8**

A solution of KSCN (0.01 mol, 0.97 g) and 1,3-choloropropionyl chloride (0.01 mol, 1.26 g) in acetone (30 mL) was refluxed for 30 minutes. The solution was left to cool then a solution of sulfanilamide **7** (0.01 mol, 1.72 g) in acetone (20 mL) was added drop wise in 15 minutes and left to stir for three hours in room temperature then 100 ml 1N HCl was added to the solution. The formed yellow precipitate was dissolved in acetone/toluene 1:1 and refluxed for six hours. The yellow precipitate formed was filtered, dried, washed with hot ethanol and crystallized from DMF/H_2O to give **8**.

Yield: 70%; m.p.: 243–245 °C; IR (KBr) (cm^{-1}): 3377-3197 (NH, NH_2), 3088-3068 (CH arom.), 2947-2926 (CH aliph.), 1689 (C=O), 1330, 1149 (SO_2); ^{1}HNMR (400 MHz, DMSO-d_6) δ: 2.76 (t, 2H, CH_2), 3.12 (t, 2H, CH_2), 6.97-7.00 (d, 2H, Ar H), 7.28 (s, 2H, NH_2SO_2, D_2O exchangeable), 7.75-7.77 (d, 2H, Ar H), 11.15 (s, 1H, NH, D_2O exchangeable); ^{13}CNMR (100.63 MHz, DMSO-d_6) δ: 23.18(1), 33.63(1), 121.73(2), 126.71(2), 139.58(1), 151.62(1), 152.71(1), 170.82(1); Anal. Calcd. for $C_{10}H_{11}N_3O_3S_2$ (Mwt. 285.34): C, 42.09; H, 3.89; N, 14.73; found C, 42.16; H, 3.92; N, 14.86.

4.1.7. General procedure for the preparation of compounds **9a-g**

A mixture of compound 8 (0.01 mol, 2.85 g) and the appropriate aldehyde (0.01 mol) was fused on oil bath for six hours. The formed mass was washed with hot ethanol, dried and crystallized form DMF/H_2O to give **9a-g**, respectively.

4.1.7.1. 4-(5-benzylidene-4-oxo-5,6-dihydro-4H-1,3-thiazin-2-ylamino)benzenesulfonamide **9a**

Yield: 52%; m.p.: 155–157 °C; IR (KBr) (cm^{-1}): 3325-3244 (NH, NH_2), 3101-3062 (CH arom.), 1689 (C=O), 1319, 1153 (SO_2); ^{1}HNMR (400 MHz, DMSO-d_6) δ: 3.45 (s, 2H, CH_2), 6.58-6.93 (m, 4H, Ar H),7.25 (s, 2H, NH_2SO_2, D_2O exchangeable), 7.50-7.99 (m, 5H, Ar H), 8.70 (s, 1H, CH=C), 10.44(s, 1H, NH, D_2O exchangeable); ^{13}CNMR (100.63 MHz, DMSO-d_6) δ: 25.55(1), 112.89(2), 119.04(2), 127.15(2), 128.27(4), 129.03(2), 130.49(2), 152.50(1), 172.78(1); Anal. Calcd. for $C_{17}H_{15}N_3O_3S_2$ (Mwt. 373.45): C, 54.67; H, 4.05; N, 11.25; found C, 54.82; H, 4.09; N, 11.34.

4.1.7.2. 4-(5-(4-Fluorobenzylidene)-4-oxo-5,6-dihydro-4H-1,3-thiazin-2-ylamino)benzene-sulfonamide **9b**

Yield: 52%; m.p.: 185–187 °C; IR (KBr) (cm^{-1}): 3336-3250 (NH, NH_2), 3097-3066 (CH arom.), 1690 (C=O), 1328, 1155 (SO_2); ^{1}HNMR (400 MHz, DMSO-d_6) δ: 3.47 (s, 2H, CH_2), 6.58-7.00 (m, 4H, Ar H), 7.24 (s, 2H, NH_2SO_2, D_2O exchangeable), 7.52-8.01 (m, 4H, Ar H), 8.70 (s, 1H, CH=C), 10.50 (s, 1H, NH, D_2O exchangeable); ^{13}CNMR (100.63 MHz, DMSO-d_6) δ: 23.30(1), 112.88(2), 116.75(2), 119.05(1), 121.72(2), 127.14(2), 127.39(2), 132.90(1), 139.58(1), 152.38(1), 171.27(1), 192.16(1); Anal. Calcd. for $C_{17}H_{14}FN_3O_3S_2$ (Mwt. 391.44): C, 52.16; H, 3.60; N, 10.73; found C, 52.34; H, 3.59; N, 10.90.

4.1.7.3. 4-(5-(4-(Dimethylamino)benzylidene)-4-oxo-5,6-dihydro-4H-1,3-thiazin-2-ylamino)-benzenesulfonamide **9c**

Yield: 52%; m.p.: 205–207 °C; IR (KBr) (cm^{-1}): 3369-3196 (NH, NH_2), 3088-3055 (CH arom.), 2920 (CH aliph.), 1697 (C=O), 1301, 1180 (SO_2); ^{1}HNMR (400 MHz, DMSO-d_6) δ: 3.13 (s, 6H, $N(CH_3)_2$), 3.47 (s, 2H, CH_2), 6.58-7.04 (m, 4H, Ar H), 7.24 (s, 2H, NH_2SO_2, D_2O exchangeable), 7.44-7.87 (m, 4H, Ar H), 8.83 (s, 1H, CH=C), 10.37 (s, 1H, NH, D_2O exchangeable); ^{13}CNMR (100.63 MHz, DMSO-d_6) δ: 23.20(1), 33.5(2), 112.05(2), 119.32(2), 121.73(2), 122.27(2), 127.39(2), 128.83(2), 134.83(1), 139.58(1), 152.84(1), 169.61(1); Anal. Calcd. for $C_{19}H_{20}N_4O_3S_2$ (Mwt. 416.52): C, 54.79; H, 4.84; N, 13.45; found C, 54.88; H, 4.89; N, 13.62.

4.1.7.4. 4-(5-(4-Bromobenzylidene)-4-oxo-5,6-dihydro-4H-1,3-thiazin-2-ylamino)benzene-sulfonamide **9d**

Yield: 55%; m.p.: 203–205 °C; IR (KBr) (cm^{-1}): 3313-3246 (NH, NH_2), 3050-3010 (CH arom.), 1678 (C=O), 1319, 1153 (SO_2); ^{1}HNMR (400 MHz, DMSO-d_6) δ: 3.47 (s, 2H, CH_2), 6.63-7.17 (m, 4H, Ar H), 7.25 (s, 2H, NH_2SO_2, D_2O exchangeable), 7.45-7.95 (m, 4H, Ar H), 8.80 (s, 1H, CH=C), 10.40 (s, 1H, NH, D_2O exchangeable); ^{13}CNMR (100.63 MHz, DMSO-d_6) δ: 23.40(1), 117.50(2), 119.24(2),

127.53(2), 128.54(1), 132.20(2), 133.43(1), 136.47(1), 139.44(1), 143.50(1), 149.00(1), 153.11(1), 171.00(1); Anal. Calcd. for $C_{17}H_{14}BrN_3O_3S_2$ (Mwt. 452.35): C, 45.14; H, 3.12; N, 9.29; found C, 45.28; H, 3.14; N, 9.34.

4.1.7.5. 4-(5-(4-Hydroxybenzylidene)-4-oxo-5,6-dihydro-4H-1,3-thiazin-2-ylamino)benzene-sulfonamide **9e**

Yield: 65%; m.p.: 272–274 °C; IR (KBr) (cm^{-1}): 3447 (OH), 3334-3228 (NH, NH_2), 3082-3057 (CH arom.), 1680 (C=O), 1327, 1155 (SO_2); ^{1}HNMR (400 MHz, DMSO-d_6) δ: 3.47 (s, 2H, CH_2), 6.63-7.00 (m, 4H, Ar H),7.28 (s, 2H, NH_2SO_2, D_2O exchangeable), 7.40-7.89 (m, 4H, Ar H), 8.81 (s, 1H, CH=C), 9.3 (s, 1H, OH, D_2O exchangeable), 10.45 (s, 1H, NH, D_2O exchangeable); ^{13}CNMR (100.63 MHz, DMSO-d_6) δ: 23.40(1), 112.89(2), 119.04(1), 121.73(2), 127.15(2), 127.39(2), 127.88(2), 128.33(1), 139.58(1), 149.00(1), 152.38(1), 172.00(1); Anal. Calcd. for $C_{17}H_{15}N_3O_4S_2$ (Mwt. 389.45): C, 52.43; H, 3.88; N, 10.79; found C, 52.59; H, 3.86; N, 10.92.

4.1.7.6. 4-(5-(4-Methoxybenzylidene)-4-oxo-5,6-dihydro-4H-1,3-thiazin-2-ylamino)benzene-sulfonamide **9f**

Yield: 68%; m.p.: 125–127 °C; IR (KBr) (cm^{-1}): 3336-3248 (NH, NH_2), 3068-3005 (CH arom.), 2966 (CH aliph.), 1680 (C=O), 1327, 1155 (SO_2); ^{1}HNMR (400 MHz, DMSO-d_6) δ: 3.35 (s, 2H, CH_2), 3.85 (s, 3H, CH_3), 6.58-6.92 (m, 4H, Ar H), 7.20 (s, 2H, NH_2SO_2, D_2O exchangeable), 7.44-7.86 (m, 4H, Ar H), 7.89 (s, 1H, CH=C), 10.34 (s, 1H, NH, D_2O exchangeable); ^{13}CNMR (100.63 MHz, DMSO-d_6) δ: 23.02(1), 55.47(1), 112.89(2), 114.13(2), 114.99(2), 119.04(2), 127.16(2), 127.88(2), 130.12(1), 130.50(1), 152.38(1), 172.55(1); Anal. Calcd. for $C_{18}H_{17}N_3O_4S_2$ (Mwt. 403.48): C, 53.58; H, 4.25; N, 10.41; found C, 53.74; H, 4.28; N, 10.49.

4.1.7.7. 4-(5-(4-Chlorobenzylidene)-4-oxo-5,6-dihydro-4H-1,3-thiazin-2-ylamino)benzene-sulfonamide **9g**

Yield: 65%; m.p.: 173–175 °C; IR (KBr) (cm^{-1}): 3345-3238 (NH, NH_2), 3097-3064 (CH arom.), 1685 (C=O), 1323, 1155 (SO_2); ^{1}HNMR (400 MHz, DMSO-d_6) δ: 3.61 (s, 2H, CH_2), 6.58-7.03 (m, 4H, Ar H), 7.33 (s, 2H, NH_2SO_2, D_2O exchangeable), 7.45-7.97 (m, 4H, Ar H), 8.80 (s, 1H, CH=C), 10.40 (s, 1H, NH, D_2O exchangeable); ^{13}CNMR (100.63 MHz, DMSO-d_6) δ: 23.00(1), 112.92(2), 119.04(2), 120.39(1), 127.16(2), 127.88(2), 129.02(1), 130.25(1), 130.53(1), 138.69(1), 142.00(1), 152.34(1), 172.00(1); Anal. Calcd. for $C_{17}H_{14}ClN_3O_3S_2$ (Mwt. 407.89): C, 50.06; H, 3.46; N, 10.30; found C, 50.23; H, 3.50; N, 10.42.

4.2. In vitro cytotoxicity screening

a. Cell culture

Human cancer cells were grown in DMEM, supplemented with 10% heat inactivated FBS, 50 units/mL of penicillin and 50 µg/mL of streptomycin and maintained at 37 °C in a humidified

atmosphere containing 5% CO_2. The cells were maintained as "monolayer culture" by serial subculturing. Normal breast cancer cells, MCF-10A, were treated similarly.

b. SRB cytotoxicity assay

Cytotoxicity was determined using SRB method as previously described by Skehan *et al*. [28] Test compounds were dissolved in DMSO and serial dilutions were used for cell treatment (0.01, 0.1, 1, 10, 100, 1000 µM). Final working DMSO concentration was kept to 1% to minimize potential cyctotoxicity therewith. Exponentially growing cells were collected using 0.25% Trypsin-EDTA and seeded in 96-well plates at 1000-2000 cells/well in supplemented DMEM. After 24 h of incubation in fresh culture medium and non-adherent cells were removed by suction. Then, adherent cells were incubated for 72 h in the presence of various concentrations of the test compounds. Following 72 h treatment, the cells were fixed with 10% trichloroacetic acid for 1 h at 4 °C. Wells were stained for 10 min at room temperature with 0.4% SRB dissolved in 1% acetic acid. The plates were air dried for 24 h and the dye was solubilized with Tris-HCl for 5 min on a shaker at 1600 rpm. The optical density (OD) of each well was measured spectrophotometrically at 564 nm with an ELISA microplate reader (ChroMate-4300, FL, USA). The following equation was employed to cancel solvent cytotoxicity: Cytotoxicity (%) = O.D. (DMSO, corrected) - O.D. (Sample, corrected) /O.D. (DMSO, corrected) * 100%. IC_{50} values were calculated according to the equation for Boltzmann sigmoidal concentration–response curve using the nonlinear regression fitting models (Graph Pad, Prism Version 5).

c. Microscopic imaging

After treatment of the cells with the investigated compounds, they were photographed by inverted microscopy (×100).

4.3. Caspase 8 and 9 assays

a. Procedure

Apoptosis is controlled by proteolytic enzymes called caspases which stimulate cell death. Caspase 8 is one of the cysteine proteases implicated in apoptosis and cytokine processing while caspase 9 is mainly responsible for activation of caspases cascade responsible for apoptosis execution. Caspases 8 and 9 activity was measured by using the colorimetric assay kit (BIOVISION, K113-25 and K119-25, respectively) following the kit assay protocol. To induce apoptosis, MCF-7 and HepG2 cell lines were incubated with the different test agents (Doxorubicin, 5-FU and **5a-d**) at their respective IC_{50} value dose for 48 h was determined. Cells were then treated with cell lysis buffer, lysate was centrifuged and the supernatant was transferred to fresh tubes. Lysate with 200 µg protein equivalent was diluted with 50 µl cell lysis buffer then 50 µl of reaction buffer (containing 10 mM DTT) was added to each sample. Finally, 5 µl of the appropriate substrate solution was added (IETD-pNA for caspase 8 and LEHD-pNA for caspase 9). After incubation at 37 ° C for 2 hr. samples were read at 400 or 405 nm.

b. Statistical analysis

Data were statistically described in terms of mean ± standard deviation (± SD). Comparison of numerical variables between the study groups was done using Mann Whitney U test for independent samples. P values less than 0.05 were considered statistically significant. All statistical calculations were done using the computer program SPSS (Statistical Package for the Social Science; SPSS Inc., Chicago, IL, USA) release 15 for Microsoft Windows.

4.4. Cell cycle analysis

To analyze cell cycle phase distribution, MCF-7 and HepG2 cells were treated with the test agents as well as by positive controls (doxorubicin and 5-FU) at their respective IC_{50} concentrations for 24 h at 37 °C in a 5% CO_2 incubator. Cells were then stained and worked with the Cytell™ Cell Cycle Kit (GE Healthcare Japan, Tokyo, Japan) and then analyzed using a Cytell™ cell imaging system (GE Healthcare Japan) according to the manufacturer's procedure.

4.5. CDK2/cyclin E1 inhibition

To assess the CDK2 activity, GST-labelled CDK2/cyclin E1 (PV6295), LanthaScreen™ Eu-anti-GST Antibody (A15116) and Kinase Tracer 236 (PV5592) from ThermoFisher Scientific were used. The assay was done according to the LanthaScreen™ Eu Kinase Binding Assay protocol developed by the manufacturer and Staurosporine was used as a positive control.

4.6. Radiolabeling and in vivo biodistribution of radioiodinated-5c

a. Radioiodinated-5c preparation

Radiolabeling technique was used as a tool to monitor the *in vivo* biodistribution of **5c**. Radiolabeling of **radioiodinated-5c** by ^{125}I was performed using the electrophilic substitution technique under oxidative conditions by chloramine-T [19-22]. Different factors that affect the radiolabeling process were studied (**5c** amount, chloramine-T amount, pH, reaction time and temperature) to reach the maximum radiochemical yield (RCY). Each factor studying experiment was performed in triplicate and one-way ANOVA test was used to evaluate data differences (level of significance set at $P<0.05$).

b. Analysis of the radiochemical yield:

Efficiency of radiolabeling and stability of **radioiodinated-5c** *in-vitro* were evaluated by ascending paper chromatography (P.C.) and TLC to determine the percent of **radioiodinated-5c** and free $^{125}I^-$ [29,30].

4.6.1. Pharmacokinetic study of radioiodinated-5c

a. Induction of cancer in mice

Induction of tumor in the right lateral thigh muscle of the Swiss albino mice was done by intramuscularly injecting 200 mL of $12.5x10^6$ cells.mL^{-1} Ehrlich ascites carcinoma. Solid tumors appeared in mice injected muscles 4-6 days after injection [19,22].

b. Biodistribution studies of the radioiodinated-5c in solid tumor bearing mice model

The animal ethics committee of Egyptian Atomic Energy Authority approved the biodistribution studies performed. Male Swiss albino mice, with body mass 20-25 g, were segregated in groups of five and fed up with food and water. Aliquots of 150 µL containing 6.2 MBq of **radioiodinated-5c** were injected intravenously in male Swiss albino mice with cancer in right thigh muscle. Mice were anaesthetized by chloroform and dissected at 15min, 1, 2 and 4 h post-injection. Each mouse was weighed and fresh blood, bone and muscle samples were separated, weighed and their radioactivities were counted. Blood, bone and muscles were calculated in percentage of 7, 10 and 40% of the total body weight, respectively [20,21]. Other body organs and tissues were also separated, weighed and their radioactivities were counted using NaI (Tl) crystal gamma counter. Percent-injected dose per organ (% ID/organ ± S.D.) at each time point for a population of five mice were reported. One-way ANOVA test was used to evaluate data differences (P<0.05).

Declaration of interest

RKA wishes to acknowledge STDF for supporting part of this research project through the grant fund provided to her “STDF 25839”.

References

[1] NIH, https://www.cancer.gov/about-cancer/understanding/statistics, last accessed 23/5/2018
[2] https://www.cancer.gov/about-cancer/treatment, last accessed 18/6/2018.
[3] M.S. Ricci, W.-X. Zong, Chemotherapeutic Approaches for Targeting Cell Death Pathways, Oncologist. 11 (2006) 342–357. doi:10.1634/theoncologist.11-4-342.
[4] https://www.mycancergenome.org/content/molecular-medicine/pathways/cytotoxic-chemotherapy-mechanisms-of-action last accessed 18/6/2018
[5] S. Elmore, Apoptosis: A Review of Programmed Cell Death, Toxicol. Pathol. 35 (2007) 495–516. doi:10.1080/01926230701320337.
[6] N.N. Danial, S.J. Korsmeyer, Cell death: critical control points., Cell. 116 (2004) 205–19.
[7] M.O. Hengartner, The biochemistry of apoptosis, Nature. 407 (2000) 770–776. doi:10.1038/35037710.
[8] T. Teitz, T. Wei, M.B. Valentine, E.F. Vanin, J. Grenet, V.A. Valentine, F.G. Behm, A.T. Look, J.M. Lahti, V.J. Kidd, Caspase 8 is deleted or silenced preferentially in childhood neuroblastomas with amplification of MYCN, Nat. Med. 6 (2000) 529–535. doi:10.1038/75007.
[9] C. Wang, R.J. Youle, The role of mitochondria in apoptosis*., Annu. Rev. Genet. 43 (2009) 95–118. doi:10.1146/annurev-genet-102108-134850.
[10] A. Casini, A. Scozzafava, A. Mastrolorenzo, L.T. Supuran, Sulfonamides and sulfonylated derivatives as anticancer agents., Curr. Cancer Drug Targets. 2 (2002) 55–75.

[11] H.I. Gul, C. Yamali, M. Bulbuller, P.B. Kirmizibayrak, M. Gul, A. Angeli, S. Bua, C.T. Supuran, Anticancer effects of new dibenzenesulfonamides by inducing apoptosis and autophagy pathways and their carbonic anhydrase inhibitory effects on hCA I, hCA II, hCA IX, hCA XII isoenzymes, Bioorg. Chem. 78 (2018) 290–297. doi:10.1016/j.bioorg.2018.03.027.

[12] A. Agudo-López, E. Prieto-García, J. Alemán, C. Pérez, C.V. Díaz-García, L. Parrilla-Rubio, S. Cabrera, C. Navarro-Ranninger, H. Cortés-Funes, J.A. López-Martín, M.T. Agulló-Ortuño, Mechanistic added value of a trans-Sulfonamide-Platinum-Complex in human melanoma cell lines and synergism with cis-Platin., Mol. Cancer. 16 (2017) 45. doi:10.1186/s12943-017-0618-7.

[13] C.-L. Guo, L.-J. Wang, Y. Zhao, H. Liu, X.-Q. Li, B. Jiang, J. Luo, S.-J. Guo, N. Wu, D.-Y. Shi, C.-L. Guo, L.-J. Wang, Y. Zhao, H. Liu, X.-Q. Li, B. Jiang, J. Luo, S.-J. Guo, N. Wu, D.-Y. Shi, A Novel Bromophenol Derivative BOS-102 Induces Cell Cycle Arrest and Apoptosis in Human A549 Lung Cancer Cells via ROS-Mediated PI3K/Akt and the MAPK Signaling Pathway, Mar. Drugs. 16 (2018) 43. doi:10.3390/md16020043.

[14] N.D. Reddy, M.H. Shoja, S. Biswas, P.G. Nayak, N. Kumar, C.M. Rao, An appraisal of cinnamyl sulfonamide hydroxamate derivatives (HDAC inhibitors) for anti-cancer, anti-angiogenic and anti-metastatic activities in human cancer cells, Chem. Biol. Interact. 253 (2016) 112–124. doi:10.1016/j.cbi.2016.05.008.

[15] A.M. Alafeefy, S.I. Alqasoumi, A.E. Ashour, M.M. Alshebly, Quinazoline-sulfonamides as potential antitumor agents: synthesis and biological testing, J. Enzyme Inhib. Med. Chem. 28 (2013) 375–383. doi:10.3109/14756366.2012.668541.

[16] A. Cumaoglu, S. Dayan, A.O. Agkaya, Z. Ozkul, N.K. Ozpozan, Synthesis and pro-apoptotic effects of new sulfonamide derivatives via activating p38/ERK phosphorylation in cancer cells, J. Enzyme Inhib. Med. Chem. 30 (2015) 413–419. doi:10.3109/14756366.2014.940938.

[17] M.M. Ghorab, M. Ceruso, M.S. Alsaid, Y.M. Nissan, R.K. Arafa, C.T. Supuran, Novel sulfonamides bearing pyrrole and pyrrolopyrimidine moieties as carbonic anhydrase inhibitors: Synthesis, cytotoxic activity and molecular modeling, Eur. J. Med. Chem. 87 (2014) 186–196. doi:10.1016/j.ejmech.2014.09.059.

[18] M.M. Ghorab, M.S. Alsaid, M. Ceruso, Y.M. Nissan, C.T. Supuran, Carbonic anhydrase inhibitors: Synthesis, molecular docking, cytotoxic and inhibition of the human carbonic anhydrase isoforms I, II, IX, XII with novel benzenesulfonamides incorporating pyrrole, pyrrolopyrimidine and fused pyrrolopyrimidine moieties., Bioorg. Med. Chem. 22 (2014) 3684–95. doi:10.1016/j.bmc.2014.05.009.

[19] T. Nasr, S. Bondock, M. Youns, Anticancer activity of new coumarin substituted hydrazide–hydrazone derivatives, Eur. J. Med. Chem. 76 (2014) 539–548. doi:10.1016/j.ejmech.2014.02.026.

[20] K.O. Mohamed, Y.M. Nissan, A.A. El-Malah, W.A. Ahmed, D.M. Ibrahim, T.M. Sakr, M.A. Motaleb, Design, synthesis and biological evaluation of some novel sulfonamide derivatives as apoptosis inducers, Eur. J. Med. Chem. 135 (2017) 424–433. doi:10.1016/j.ejmech.2017.04.069.

[21] T. Sakr, M. Khedr, H. Rashed, M. Mohamed, In Silico-Based Repositioning of Phosphinothricin as a Novel Technetium-99m Imaging Probe with Potential Anti-Cancer Activity, Molecules. 23 (2018) 496. doi:10.3390/molecules23020496.

[22] R.I. Al-Wabli, T.M.M.H. Sakr, M.A. Khedr, A.A. Selim, M.A.E.-M.A. El-Rahman, W.A. Zaghary, Platelet-12 lipoxygenase targeting via a newly synthesized curcumin derivative radiolabeled with technetium-99m., Chem. Cent. J. 10 (2016) 73. doi:10.1186/s13065-016-0220-x.

[23] A.-M. Monforte, S. Ferro, L. De Luca, G. Lo Surdo, F. Morreale, C. Pannecouque, J. Balzarini, A. Chimirri, Design and synthesis of N1-aryl-benzimidazoles 2-substituted as novel HIV-1 non-nucleoside reverse transcriptase inhibitors, Bioorg. Med. Chem. 22 (2014) 1459–1467. doi:10.1016/j.bmc.2013.12.045.

[24] M.G. Assy, REACTION OF ACYL ISOTHIOCYANATES WITH NUCLEOPHILES: A CONVENIENT SYNTHESIS OF 1,3-OXAZINE, PYRIMIDINETHIONE AND THIAZOLE DERIVATIVES, Phosphorus.

Sulfur. Silicon Relat. Elem. 108 (1996) 15–20. doi:10.1080/10426509608029633.
[25] D.S. Mansuroğlu, H. Arslan, D. VanDerveer, G. Binzet, Synthesis and Characterization of *N* -(2,2-Diphenylacetyl)- *N* '-Substituted Thiourea Derivatives: The Crystal Structure of *N* -(2,2-Diphenylacetyl)- *N* '-(4-chloro phenyl)-thiourea, Phosphorus. Sulfur. Silicon Relat. Elem. 184 (2009) 3221–3230. doi:10.1080/10426500902979743.
[26] P. Skehan, R. Storeng, D. Scudiero, A. Monks, J. McMahon, D. Vistica, J.T. Warren, H. Bokesch, S. Kenney, M.R. Boyd, New colorimetric cytotoxicity assay for anticancer-drug screening., J. Natl. Cancer Inst. 82 (1990) 1107–12.
[27] M. Payton, G. Chung, P. Yakowec, A. Wong, D. Powers, L. Xiong, N. Zhang, J. Leal, T.L. Bush, V. Santora, B. Askew, A. Tasker, R. Radinsky, R. Kendall, S. Coats, Discovery and Evaluation of Dual CDK1 and CDK2 Inhibitors, Cancer Res. 66 (2006) 4299–4308. doi:10.1158/0008-5472.CAN-05-2507.
[28] T.M. Sakr, M.H. Sanad, W.H. Abd-Alla, D.H. Salama, G.M. Saleh, Radioiodinated esmolol as a highly selective radiotracer for myocardial perfusion imaging: In silico study and preclinical evaluation, Appl. Radiat. Isot. 137 (2018) 41–49. doi:10.1016/j.apradiso.2018.03.006.
[29] T.M. Sakr, I.T. Ibrahim, W.H. Abd-Alla, Molecular modeling and preclinical evaluation of radioiodinated tenoxicam for inflammatory disease diagnosis, J. Radioanal. Nucl. Chem. 316 (2018) 233–246. doi:10.1007/s10967-018-5770-z.
[30] M.M. Swidan, T.M. Sakr, M.A. Motaleb, A. Abd El-Bary, M.T. El-Kolaly, Preliminary assessment of radioiodinated fenoterol and reproterol as potential scintigraphic agents for lung imaging, J. Radioanal. Nucl. Chem. 303 (2015) 531–539. doi:10.1007/s10967-014-3328-2.
[31] T.A. Chohan, H. Qian, Y. Pan, J.-Z. Chen, Cyclin-dependent kinase-2 as a target for cancer therapy: progress in the development of CDK2 inhibitors as anti-cancer agents., Curr. Med. Chem. 22 (2015) 237–63.
[32] X. Yin, J. Yu, Y. Zhou, C. Wang, Z. Jiao, Z. Qian, H. Sun, B. Chen, Identification of CDK2 as a novel target in treatment of prostate cancer, Futur. Oncol. 14 (2018) 709–718. doi:10.2217/fon-2017-0561.

Graphical abstract

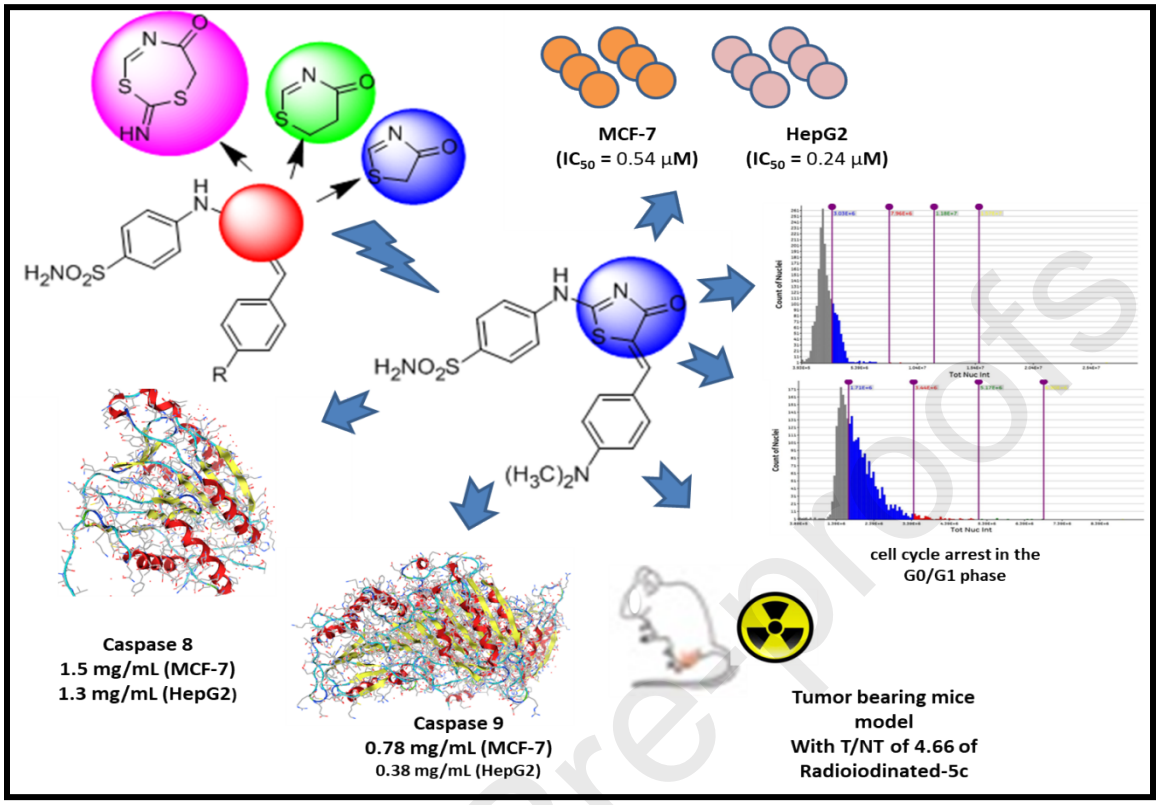

Highlights

- New thiazolidinone, thiazinone and dithiazepinone-benzenesulfonamides as cytotoxic agents.
- Effect of **5a-d** on MCF-7 and HepG2 cell cycle phase distribution.
- Caspase 8 and 9 levels determination in MCF-7 and HepG2 after test agents' treatment.
- *In vivo* biodistribution study of **radioiodinated-5c.**

Conflict of interest

RKA wishes to acknowledge STDF for supporting part of this research project through the grant fund provided to her "STDF 25839".